

COVER PAGE

Document downloaded by @DAEL

Fri Nov 27 18:29:07 2026

For personal use

When automatic English translation is provided, only the original document is authentic.

The EAA cannot be held responsible of any translation error

Bibliographical reference

On the Influence of Obstacle Modeling in Multiple Diffraction of Acoustic Waves, Domingo Pardo-Quiles, José-Víctor Rodríguez, Rubén Lozano-Giménez, Leandro Juan-Llácer and Juan Pascual-García, Acta Acustica **vol. 105** (Number 2), 2019, pp. 261-264

DOI

https://doi.org/10.3813/AAA.919308

Acta Acustica united with Acustica
Vol. 105 (2019) 261 – 264

DOI 10.3813/AAA.919308

On the Influence of Obstacle Modeling in Multiple Diffraction of Acoustic Waves

Domingo Pardo-Quiles, José-Víctor Rodríguez, Rubén Lozano-Giménez, Leandro Juan-Llácer, Juan Pascual-García

Departamento de Tecnologías de la Información y las Comunicaciones. Universidad Politécnica de Cartagena. Antiguo Cuartel de Antiguones, Plaza del Hospital, 1 30202 Cartagena, Murcia, Spain. domingo.pardo@upct.es

Summary

Two uniform theory of diffraction (UTD)-based formulations for the analysis of the multiple diffraction of sound when the diffracting obstacles are modeled as both rectangular sections and cylinders are hereby presented. More realistic models are proposed while at the same time the insertion losses results are compared with those obtained with a formulation already published which assumes the obstacles to be modeled as knife-edges or wedges. In this way, an analysis of the impact of obstacle modeling on sound attenuation is carried out, thus contributing to obtaining more precise acoustic propagation models when multiple diffraction caused by equi-spaced objects of rectangular or cylindrical shape has to be taken into account.

PACS no. 43.20.Dk, 43.20.Rl, 43.20.Gp, 43.20.Ye, 43.30.Vh, 43.30.Wi, 43.30.Xm, 43.30.Yj, 43.58.Bh

1. Introduction

Analysis of the acoustic wave diffraction caused by multiple obstacles has been carried out by means of a set of works and formulations, which can be based on Boundary Element Methods (BEM) [1], Parabolic Equation Methods (PEM) [2], Geometric Theory of Diffraction (GTD) [3, 4, 5], as well as empirical formulae [6]. In this respect, the study of the multiple diffraction of acoustic waves can be of special relevance in environments where a set of identical diffraction obstacles are evenly spaced, as happens with the rows of seats in common auditoriums or concert halls. In this way, some of the abovementioned authors have recently published a work [5] where a two-dimensional (2D) uniform theory of diffraction (UTD)-based formulation for such a type of environment is proposed. In this theoretical model, thanks to its recursivity, an excess use of the UTD within the transition zone (along the shadow boundary) can be avoided. In this way, the constraints of former works when the diffracting elements have the same height are solved, as well as substantially reducing the computation time required, mainly when a high number of obstacles is considered.

The proposed formulation in [5] specifically considers the modeling of diffracting obstacles as knife-edges or wedges. However, if more realistic and precise propagation results are to be obtained, additional formulations considering obstacles modeled as rectangular sections or cylinders should be achieved. This could lead to a closer approach to the shape of the seats (rectangular) used in the already mentioned acoustic environments or to the diffracting heads of the audience (cylinders) when such auditoriums or concert halls are full of people.

Therefore, in this paper, two UTD-based formulations for the acoustic diffraction analysis of arrays of rectangular sections or cylinders, –based on hybrid UTD-physical optics (PO) theoretical models applied in the diffraction of electromagnetic waves– are proposed. In this way, a comparison of the insertion losses results obtained by means of the four different models (knife-edges, wedges, rectangular sections, and cylinders) will be carried out. This will allow us to assess the impact of the type of obstacle modeling on acoustic multiple- diffraction results.

2. Propagation environment

In Figure 1, the different propagation schemes considered are shown, in which four different obstacle models for the n diffraction obstacles have been assumed: a) knife-edges, b) wedges with inner angle γ, c) rectangular sections of width v, and d) cylinders with radius r. In this sense, $\phi(n)$ is the acoustic field reaching the receivers in models a), b), d), but, on the contrary, is the acoustic field located in the corners on the right of the rectangular sections of model c). For the latter, the acoustic field reaching the receiver is expressed by ϕ_n. In all cases, obstacles have been considered to be absorbent, with the same height, and evenly spaced by a distance w (in the case of rectangular sections, $w = v + w'$ and, in the case of cylinders, $2r = v$). Moreover, the source of transmission is placed at a distance d from the first obstacle (in such a way that the spherical wave impinges on the first obstacle with an angle α) and

Received 11 October 2018,
accepted 19 December 2018.

© S. Hirzel Verlag · EAA

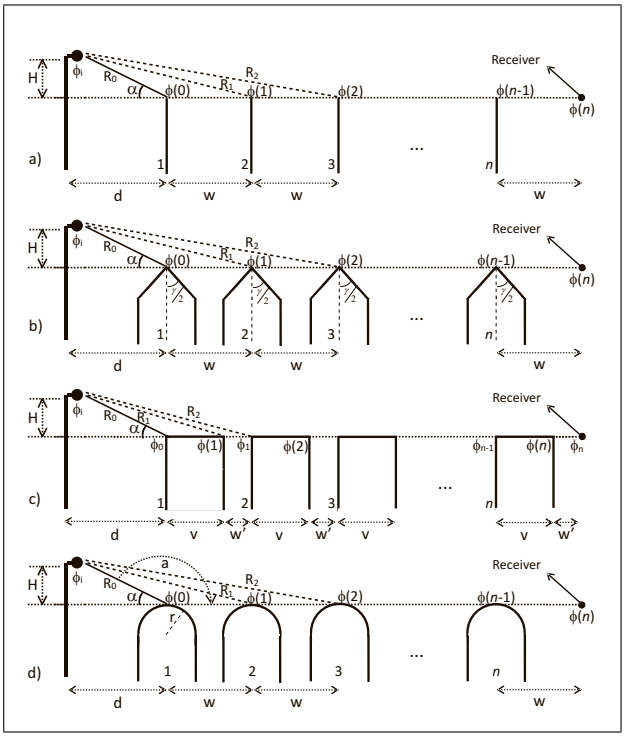


Figure 1. Propagation schemes considered for a) edges, b) wedges c) rectangular sections, and d) cylinders.

height H with respect to the height of the diffracting elements. Finally, the receiver is placed at the same height as the obstacles and at a range of w from the last one (in the case of rectangular sections, the distance from the right corner of the last block has been assumed as w' so that the total distance traveled by the wave in all cases is $d + nw$). It should be noted that this position of the receiver corresponds to the point at which a hypothetical listener would be placed after n rows of equi-spaced seats in an auditorium or concert hall.

3. Theoretical Method

The formulation considered for the calculation of the acoustic field at the receiving point $\phi(n)$ for the cases of knife-edges and wedges is the one already proposed by the authors in [5]. The new formulations for rectangular sections and cylinders are proposed below.

3.1. Obstacles modeled as rectangular sections

By considering the formulation published in [7] by the authors for the analysis of the multiple diffraction of electromagnetic waves caused by rectangular objects, if we assume the acoustic field that reaches the left corner of the first rectangular obstacle of Figure 1c as

$$\phi_0 = \frac{\phi^i}{R_0} \exp\left(-\mathrm{j}kR_0\right), \tag{1}$$

ϕ^i being the relative amplitude of a spherical source and k the wave number, the total acoustic field that reaches the receiver point ϕ_n can be calculated, assuming $\alpha \geq 0$ and $n \geq 1$, as

$$\begin{aligned}\phi_n = \frac{1}{2n}\Bigg\{ & \sum_{q=0}^{n-1} \phi_q \Bigg[\frac{R_0}{R_{2(n-q)}} \exp\left(-\mathrm{j}k(R_{2n} - R_{2q})\right) \\ & + \sqrt{\frac{R_0}{(n-q)(v+w')\left[R_0 + (n-q)(v+w')\right]}} \\ & \cdot D\Bigg(\varphi' = \pi/2 + \alpha, \varphi = 3\pi/2, \\ & \qquad L = \sqrt{\frac{R_0(n-q)(v+w')}{R_0 + (n-q)(v+w')}}\Bigg) \\ & \cdot \exp\left(-\mathrm{j}k(n-q)(v+w')\right)\Bigg] \\ & + \sum_{r=1}^{n} \phi(r) \Bigg[\frac{R_0}{R'_{2(n-r)+1}} \exp\left(-\mathrm{j}k(R_{2n} - R_{2r-1})\right) \\ & + \sqrt{\frac{R_0}{\left[(n-r)(v+w') + w'\right]\left[R_0 + (n-r)(v+w') + w'\right]}} \\ & \cdot D\Bigg(\varphi' = \alpha, \varphi = \pi, \\ & \qquad L = \sqrt{\frac{R_0\left[(n-r)(v+w') + w'\right]}{R_0 + \left[(n-r)(v+w') + w'\right]}}\Bigg) \\ & \cdot \exp\left(-\mathrm{j}k[(n-r)(v+w') + w']\right)\Bigg]\Bigg\}, \end{aligned} \tag{2}$$

where $D(\varphi, \varphi', L)$ is the diffraction coefficient proposed in [8] for knife-edges/wedges,

$$\begin{aligned} R_x &= \begin{cases} \sqrt{\left(d + \frac{x}{2}(v+w')\right)^2 + H^2}, & x \text{ even}, \\ \sqrt{\left(d + \frac{x-1}{2}(v+w') + v\right)^2 + H^2}, & x \text{ odd}, \end{cases} \\ R'_x &= \sqrt{\left(d + \frac{x-1}{2}(v+w') + w'\right)^2 + H^2}, \end{aligned} \tag{3}$$

and, as previously mentioned, $\phi(n)$ is the acoustic field located in the corners on the right of the rectangular sections, which can be expressed as

$$\begin{aligned}\phi(n) = & \\ \frac{1}{2n-1}\Bigg\{ & \sum_{m=0}^{n-1} \phi_m \Bigg[\frac{R_0}{R_{2(n-m)-1}} \exp\left(-\mathrm{j}k(R_{2n-1} - R_{2m})\right) \\ & + \sqrt{\frac{R_0}{\left[(n-m)(v+w') - w'\right]\left[R_0 + (n-m)(v+w') - w'\right]}} \\ & \cdot D\Bigg(\varphi' = \pi/2 + \alpha, \varphi = 3\pi/2, \\ & \qquad L = \sqrt{\frac{R_0(n-m)(v+w') - w'}{R_0 + (n-m)(v+w') - w'}}\Bigg) \\ & \cdot \exp\left(-\mathrm{j}k[(n-m)(v+w') - w']\right)\Bigg] \end{aligned}$$

$$\cdot \sum_{p=1}^{n-1} \phi(p) \left[\frac{R_0}{R'_{2(n-p)}} \exp\left(-\mathrm{j}k(R_{2n-1} - R_{2p-1}) \right) + \sqrt{\frac{R_0}{(n-p)(v+w')\left[R_0 + (n-p)(v+w')\right]}} \cdot D\left(\varphi' = \alpha, \varphi = \pi, L = \sqrt{\frac{R_0\left[(n-p)(v+w')\right]}{R_0 + \left[(n-p)(v+w')\right]}} \right) \cdot \exp\left(-\mathrm{j}k(n-p)(v+w') \right) \right] \Bigg\}. \quad (4)$$

3.2. Obstacles modeled as cylinders

By considering the formulation published in [9] by the authors for the analysis of the multiple diffraction of electromagnetic waves caused by cylindrical objects, if we consider $\alpha \geq 0$ and $n \geq 1$, the acoustic field reacting the receiver in Figure 1d can be expressed as

$$\phi(n) = \frac{1}{n} \sum_{m=0}^{n-1} \phi(m) \left[\frac{R_0}{R_{(n-m)}} \mathrm{e}^{-\mathrm{j}k(R_n - R_m)} + \sqrt{\frac{R_0}{(n-m)w\left[R_0 + (n-m)w\right]}} \cdot R_{s,h}(a) \exp\left(-\mathrm{j}k(n-m)w \right) \right] \quad (5)$$

where

$$\phi(0) = \frac{\phi^i}{R_0} \mathrm{e}^{-\mathrm{j}kR_0} \quad (6)$$

is the field that impinges on the first cylinder, being that ϕ^i is the relative amplitude of a spherical source and k is the wave number, and

$$R_{s,h}(a) = -\sqrt{\frac{r}{m'}} \mathrm{e}^{-\mathrm{j}\varepsilon^3(a)/12} \mathrm{e}^{-\mathrm{j}\pi/4} \cdot \left\{ \frac{-F\left[X(a)\right]}{2\varepsilon(a)\sqrt{\pi}} + q^*\left(\varepsilon(a)\right) \right\} \quad (7)$$

is the reflection coefficient where $F[X]$ is the so-called transition function, which is defined in terms of a Fresnel integral,

$$F[x] = 2\mathrm{j}\sqrt{x}\mathrm{e}^{\mathrm{j}x} \int_{\sqrt{x}}^{\infty} \mathrm{e}^{-\mathrm{j}u^2} \mathrm{d}u. \quad (8)$$

$q^*(\varepsilon(a))$ is the Fock scattering function [10],

$$q^*(x) = \frac{1}{2\sqrt{\pi}x} + \frac{1}{\sqrt{\pi}} \int_{-\infty}^{\infty} \frac{V'(t)}{w'_2(t)} \mathrm{e}^{-\mathrm{j}xt} \mathrm{d}t \quad (9)$$

(the prime represents differentiation with respect to argument), where $V(t)$ and $w_2(t)$ are defined as

$$V(t) = \sqrt{\pi} A_i(t), \quad (10)$$

$$w_2(t) = 2\sqrt{\pi}\mathrm{e}^{-\mathrm{j}\pi/6} A_i\left(t\mathrm{e}^{-\mathrm{j}2\pi/3}\right), \quad (11)$$

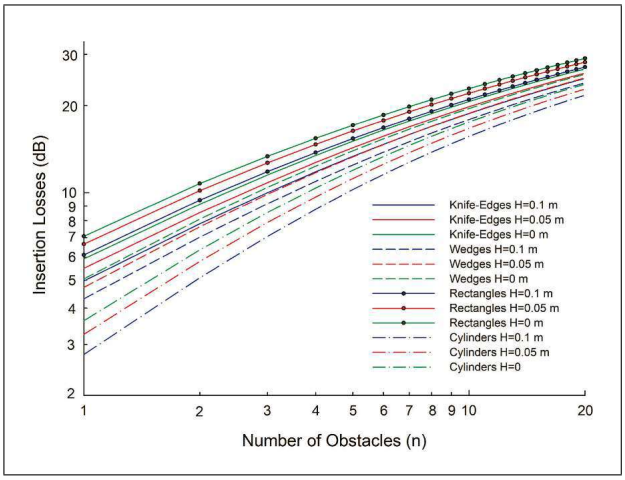


Figure 2. Insertion losses for different modeling and values of H. $f = 500\,\mathrm{Hz}$, $d = w = 1\,\mathrm{m}$, $\gamma = 60°$, $v = 0.2\,\mathrm{m}$, $w' = 0.8\,\mathrm{m}$, and $r = 0.1\,\mathrm{m}$.

with $A_i(t)$ as a Miller-type Airy function,

$$A_i(t) = \frac{1}{\pi} \int_0^{\infty} \cos\left(\frac{1}{3}zs + tz \right) \mathrm{d}z \quad (12)$$

and

$$X(a) = 2kL\cos^2\left(\frac{a}{2}\right), \quad L = \frac{R_0(n-m)w}{R_0 + (n-m)w}, \quad \varepsilon(a) = -2m'\cos\left(\frac{a}{2}\right), \quad (13)$$

where a (dependent on α) is the angle indicated in Figure 1d and $m' = (kr/2)^{1/3}$.

4. Results

Figures 2 and 3 represent, as a function of the number of obstacles considered (n) and for different values of H, the so-called insertion losses (IL), which refer to the attenuation caused by the presence of the diffraction elements, and can be defined, for the knife-edges/wedges/cylinders case, as

$$\mathrm{IL(dB)} = -20\log_{10}\left(\left| \frac{\phi(n)}{\phi_{fs}} \right| \right) \quad (14)$$

and, if rectangular sections are assumed, as

$$\mathrm{IL(dB)} = -20\log_{10}\left(\left| \frac{\phi_n}{\phi_{fs}} \right| \right), \quad (15)$$

where ϕ_{fs} represents the acoustic field received in free space (considering an absence of obstacles). In both figures, the shared parameters of $d = w = 1\,\mathrm{m}$, $\gamma = 60°$, $v = 0.2\,\mathrm{m}$, $w' = 0.8\,\mathrm{m}$, $r = 0.1\,\mathrm{m}$, and frequencies (f) of 500 Hz for Figure 2 and of 2000 Hz for Figure 3 have been taken into account.

As can be seen, the difference in modeling has a clear impact on the insertion losses obtained. Specifically, it

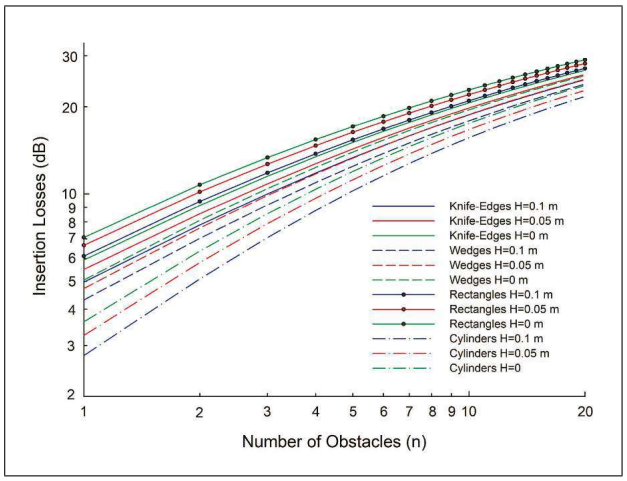


Figure 3. Insertion losses for different modeling and values of H. $f = 2000\,\text{Hz}$, $d = w = 1\,\text{m}$, $\gamma = 60°$, $v = 0.2\,\text{m}$, $w' = 0.8\,\text{m}$, and $r = 0.1\,\text{m}$.

can be seen how, on the one hand, the difference between knife-edges and wedges increases –with the edges always having greater losses– as both the number of obstacles (n) and the incident angle α decrease (with the trend remaining until $n = 7$ for the case of n). Moreover, such difference between knife-edges and wedges also decreases at a lower frequency, this difference reaching a maximum of 1.12 dB for $H = 0$, $n = 7$ and $f = 500\,\text{Hz}$.

On the other hand, the losses generated by the rectangular sections are the highest of all in both frequencies, increasing, in this case, the difference with the modeling of knife-edges at a higher frequency, a lower angle of incidence, and as the number of considered obstacles increases. The biggest difference in this respect is reached for $f = 2000\,\text{Hz}$, $H = 0$ and $n = 20$, with 2.75 dB.

Finally, regarding the attenuation caused by cylinders, it should be noted that it is, in general, the lowest of all cases (except for $f = 2000\,\text{Hz}$ and $H = 0$). The fact that this modeling produces the lowest losses due to multiple diffraction can be explained if we consider that, since $\alpha \geq 0$, the receiver considered in Figure 1d is in the so-called *Lit Region*, and therefore the acoustic field scattered by the surface of the cylinders is a reflected field instead of a diffracted field (the coefficient expressed in (8) is actually a reflection coefficient, not a diffraction one). The interesting point is that such coefficient is expressed as a function of the summation of two parameters: the first parameter represents the Fresnel diffraction process but the second one takes into account the effect of the so-called 'creeping waves', which are generated by the Fock currents on the surface of the cylinders. Thus, the total scattered energy at the cylinders is less attenuated and more focused towards the receiver than in the rest of the models, where a pure diffraction phenomenon caused by sharp obstacles takes place. The difference with respect to knife-edges is greater at $f = 500\,\text{Hz}$ than at $f = 2000\,\text{Hz}$, and a maximum arises at around $n = 82$ for both frequencies and the three values of H considered (with the highest difference of 3.14 dB –with the knife-edges causing more attenuation– at $f = 500\,\text{Hz}$, $H = 0.1\,\text{m}$, and $n = 8$).

5. Conclusions

In this article, two UTD-based formulations for the analysis of multiple sound diffraction caused by a series of obstacles modeled as rectangular sections and cylinders have been proposed. In this way, it has been possible to make a comparison between the results obtained for such models and the cases in which the diffraction elements are modeled as knife-edges and wedges. Therefore, we have been able to carry out an analysis of the impact that the modeling of the objects can have on multiple sound diffraction studies. In view of the results, it can be concluded that the manner in which the obstacles are modeled has a clear impact on the insertion losses obtained, with the rectangular sections causing the most attenuation and the cylinders the least. The maximum difference between the rectangles and the knife-edges is reached for $f = 2000\,\text{Hz}$, $H = 0$ and $n = 20$, with 2.75 dB, and the maximum difference between knife-edges and cylinders is obtained for $f = 500\,\text{Hz}$, $H = 0.1\,\text{m}$, and $n = 8$, with 3.14 dB.

Acknowledgement

This work was supported by the Ministerio de Economía y Competitividad (MINECO), Spain (TEC2016-78028-C3-2-P) and in part by European FEDER Funds.

References

[1] R. Seznec: Diffraction of sound around barriers: use of the boundary elements technique. Journal of Sound and Vibration **73** (1980) 195–209.

[2] E. M. Salomons: Diffraction by a screen in downwind sound propagation: A parabolic-equation approach. J. Acoust. Soc. Am. **95** (1994) 3109.

[3] H. S. Kim, J. S. Kim, H. J. Kang, B. K. Kim, S. R. Kim: Sound diffraction by multiple wedges and thin screens. Appl. Acoust. **66** (2005) 1102–1119.

[4] H. Min, X. Qiu: Multiple acoustic diffraction around rigid parallel wide barriers. J. Acoust. Soc. Am. **126** (2009) 179–186.

[5] J.-V. Rodríguez, J. Pascual-García, M.-T. Martínez-Inglés, J.-M. Molina-Garcia-Pardo., L. Juan-Llácer: Uniform theory of diffraction (UTD)-based solution for sound diffraction caused by an array of obstacles. J. Acoust. Soc. Am. **142**(2) (2017), 902–907.

[6] U. J. Kurze, G. S. Anderson: Sound attenuation by barriers, Appl. Acoust. **4** (1971), 35–53.

[7] M.-T. Martínez-Inglés, J-V. Rodríguez, J-M. Molina-Garcia-Pardo, J. Pascual-García, L. Juan-Llácer: Comparison of a UTD-PO Formulation for Multiple-Plateau Diffraction with Measurements at 62 GHz. IEEE Trans. on Antennas and Propagation **61** (2013). 1000–1003.

[8] R. G. Kouyoumjian, P. H. Pathak: A uniform geometrical theory of diffraction for an edge in a perfectly conducting surface. Proc. IEEE **62** (1974) 1448–1461.

[9] J.-V. Rodríguez, J.-M. Molina-Garcia, L.-J. Llácer: A Hybrid UTD-PO Solution for Multiple-Cylinder Diffraction Analysis Assuming Spherical-Wave Incidence. IEEE Trans. on Antennas and Propagation **56** (2008) 3078–3081.

[10] D. A. McNamara, C. W. I. Pistorius, J. A. G. Malherbe: Introduction to the uniform geometrical theory of diffraction. Artech House, Norwood, MA, (1990).